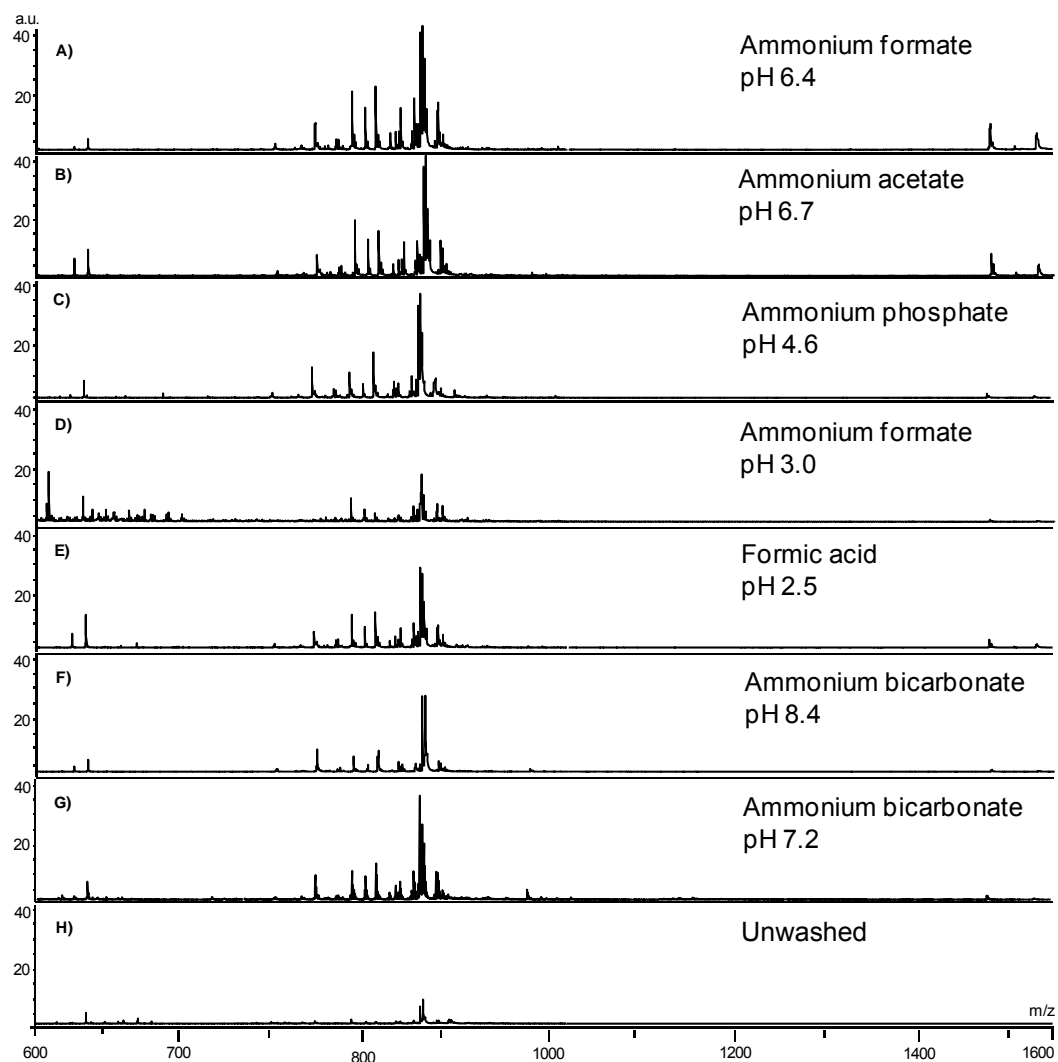


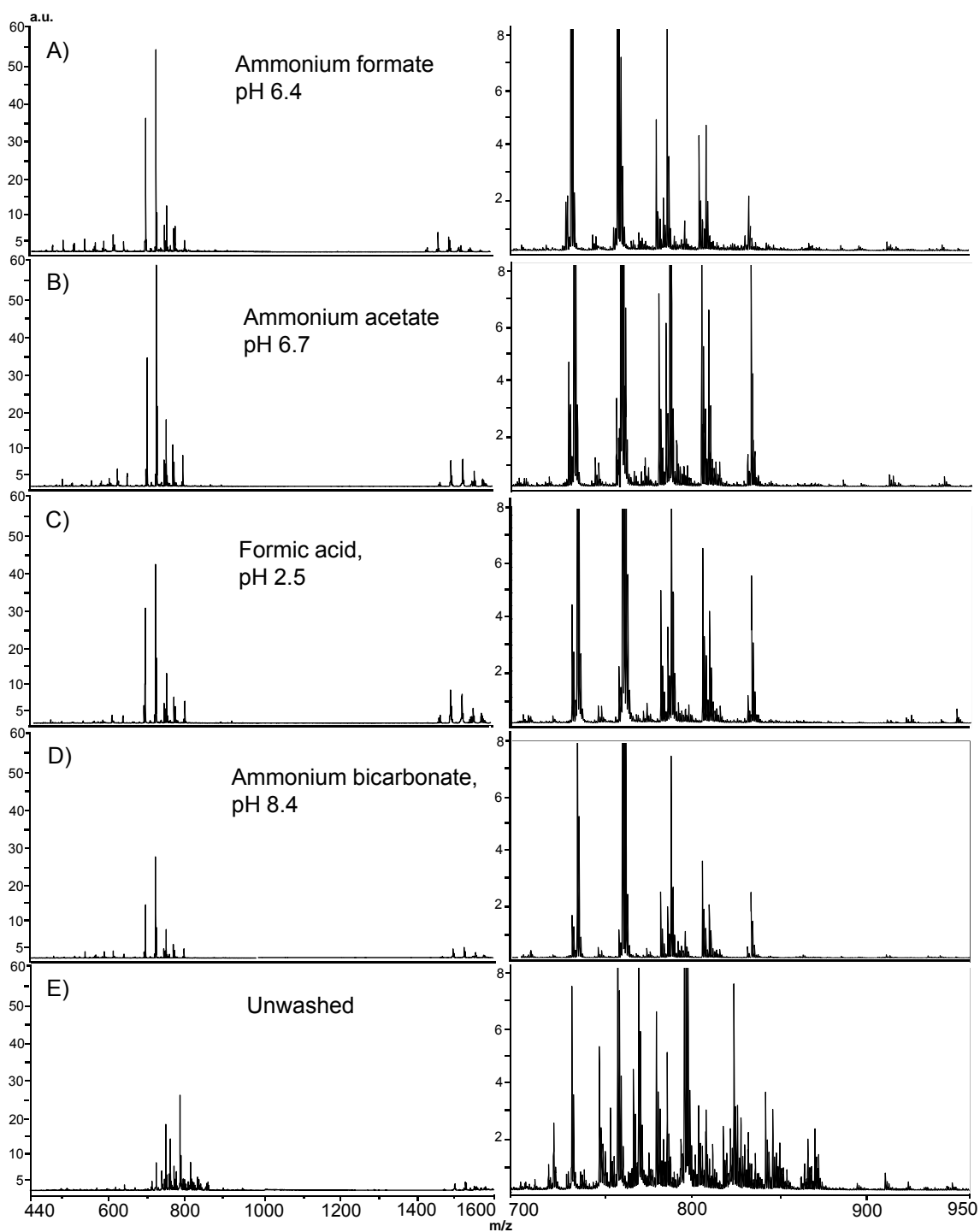
SUPPLEMENTARY FIGURES

Supplemental Figure 1



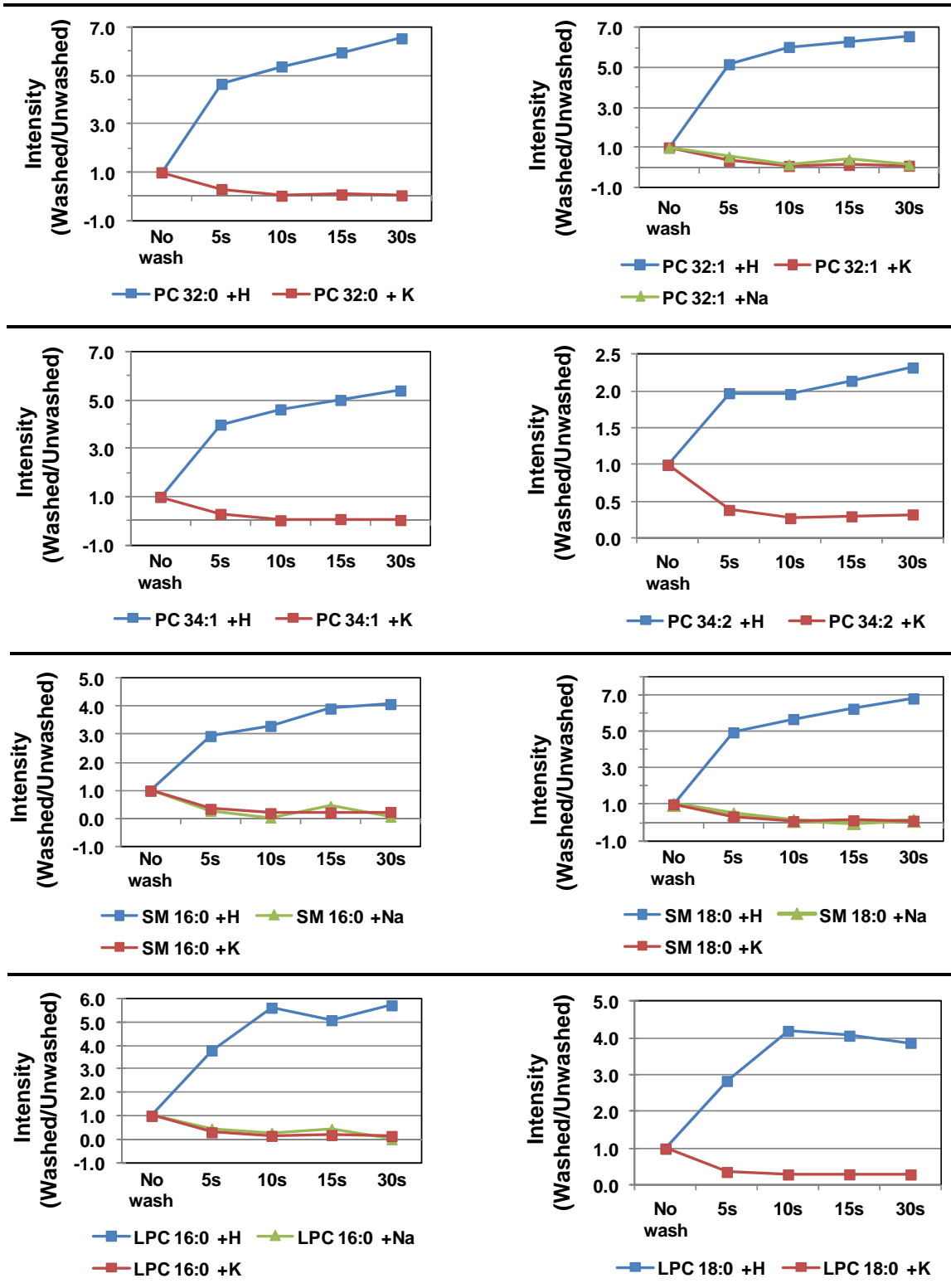
Supplemental Figure 1: Overall average mass spectrum from thin tissue sections (12 μm) analyzed in negative ion mode. Each section was washed for 15 seconds with select buffers prepared at a 50 mM concentration followed by application of the matrix 2,5 DHB by sublimation. A) ammonium formate, pH 6.4; B) ammonium acetate, pH 6.7; C) ammonium phosphate, pH 4.6; D) ammonium formate, pH 2.5; E) formic acid, pH 2.5; F) ammonium bicarbonate, pH 8.4; G) ammonium bicarbonate, pH 7.2; H) Control (unwashed section).

Supplemental Figure 2



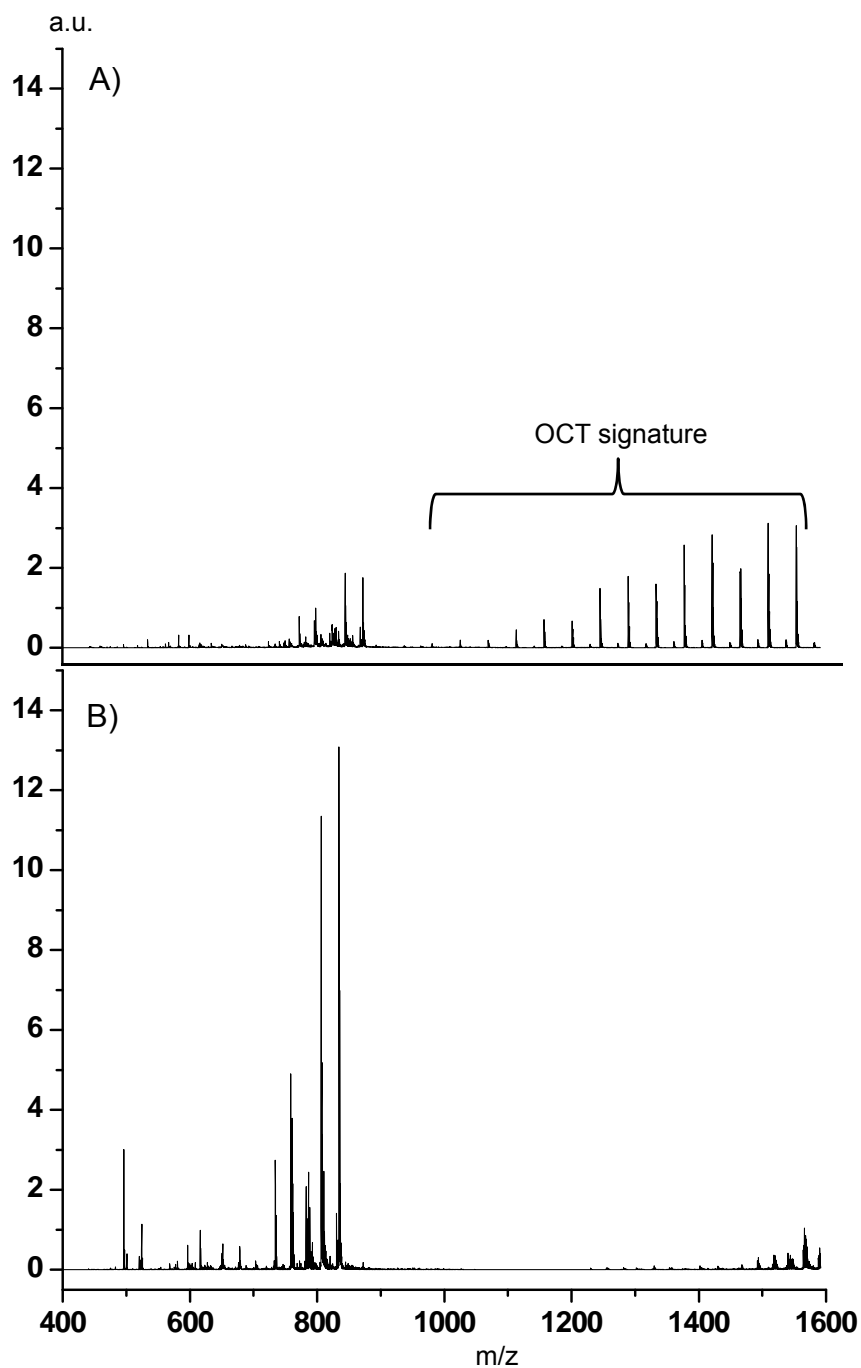
Supplemental Figure 2: Overall average mass spectrum from thin tissue sections (12 μm) analyzed in positive ion mode. Each section was washed for 15 seconds with select buffers prepared at a 50 mM concentration followed by application of the matrix 2,5 DHB by sublimation. A) ammonium formate, pH 6.4; B) ammonium acetate, pH 6.7; C) ammonium formate, pH 3.0; E) formic acid, pH 2.5; D) ammonium bicarbonate, pH 8.4; E) Control (unwashed section).

Supplemental Figure 3



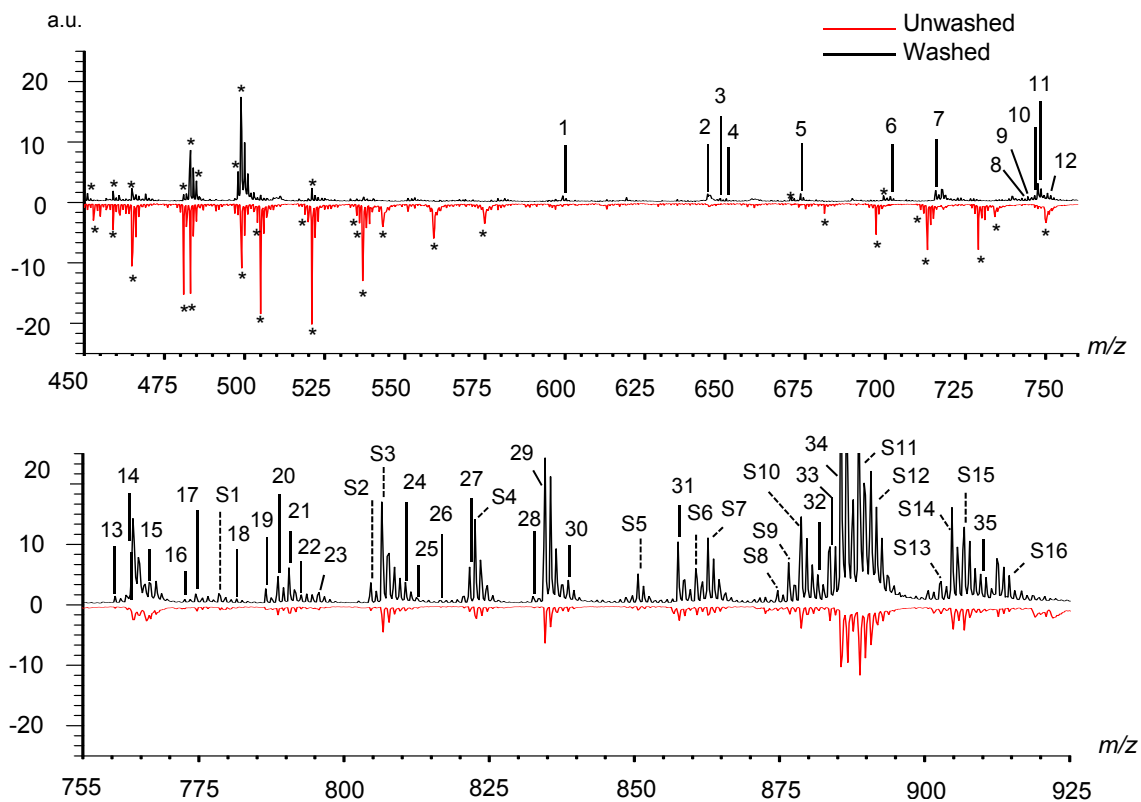
Supplemental Figure 3: The effects of washing on positive ion mode analysis. Examples of average signal increase for M+H peaks of glycerophosphocholines and sphingomyelins analyzed in positive ion mode after tissue washing for specified times with 50 mM ammonium formate.

Supplemental Figure 4



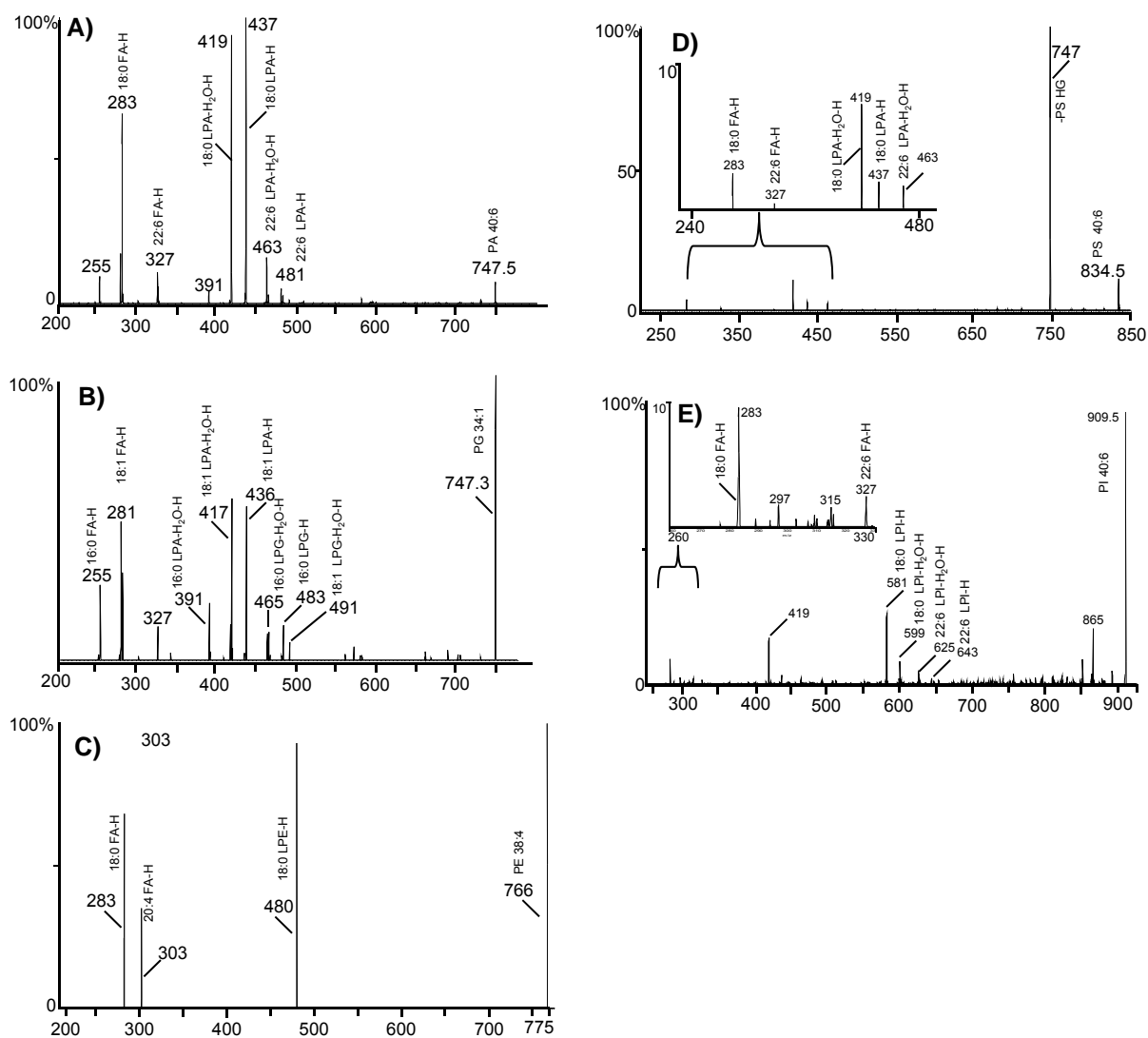
Supplemental Figure 4: Comparison of positive mode spectra before and after washing from tissue embedded in optimal cutting temperature (OCT) media. Tissue was washed for two times 15 seconds in 4°C 50 mM ammonium formate, pH 6.4 followed by drying under vacuum. A) Before washing treatment; B) After washing treatment

Supplemental Figure 5



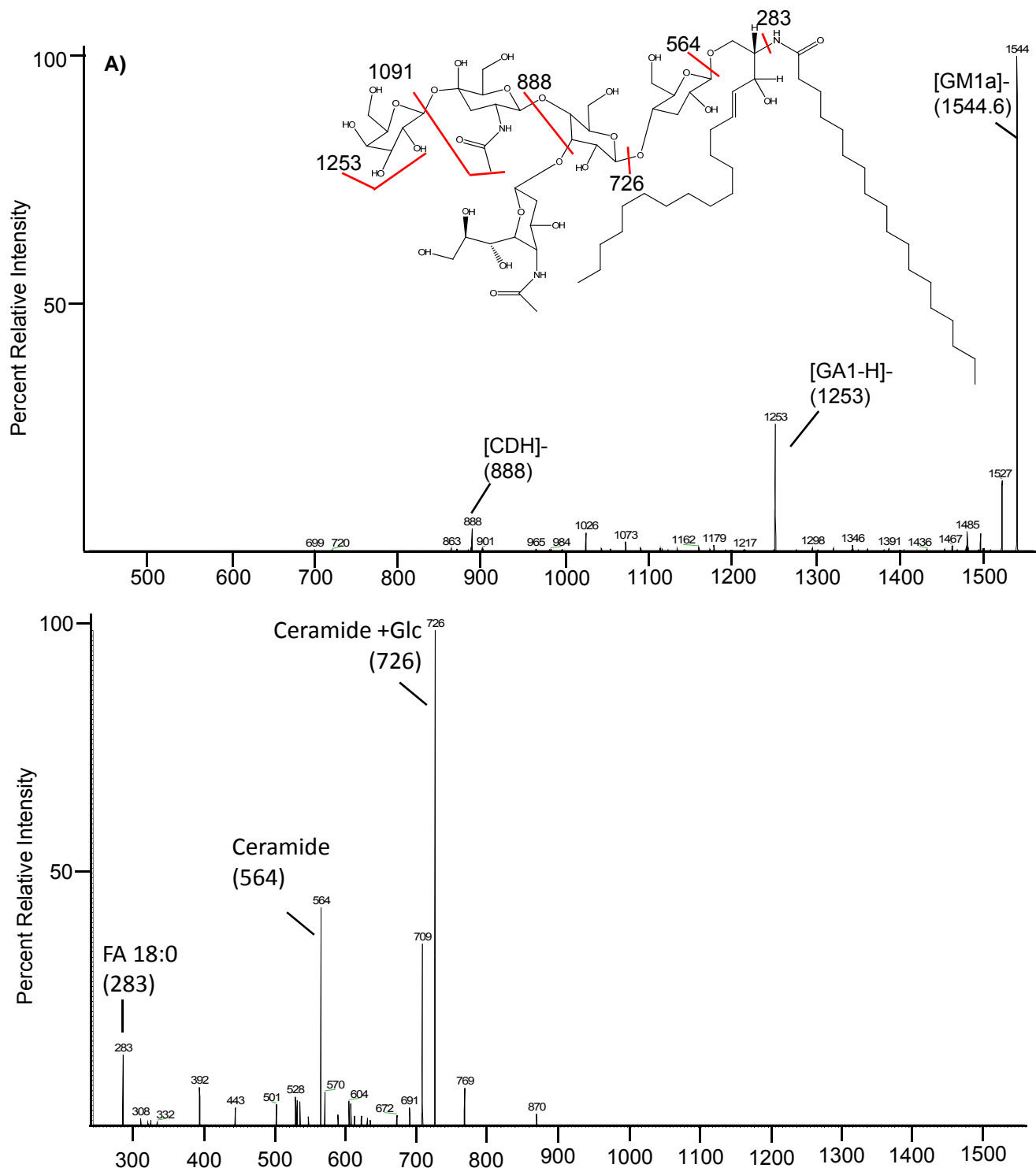
Supplemental Figure 5. Comparison of total ion current m/z range 450-925. Numbers correspond to lipid species referenced in Supplemental Table 1; sulfatide numbers are prefixed by the letter S; *- matrix cluster.

Supplemental Figure 6



Supplemental Figure 6. On-tissue fragmentation of glycerophospholipids by MALDI linear ion trap (Thermo Scientific, Waltham, MA, USA). A) GPA (18:0/22:6), adult mouse brain; B) GPG (16:0/18:1) from liver tissue, P0 mouse; C) GPE 18:0/20:4, adult mouse brain; D) GPS (18:0/22:6), adult mouse brain; E) GPI (18:0/22:6), adult mouse brain.

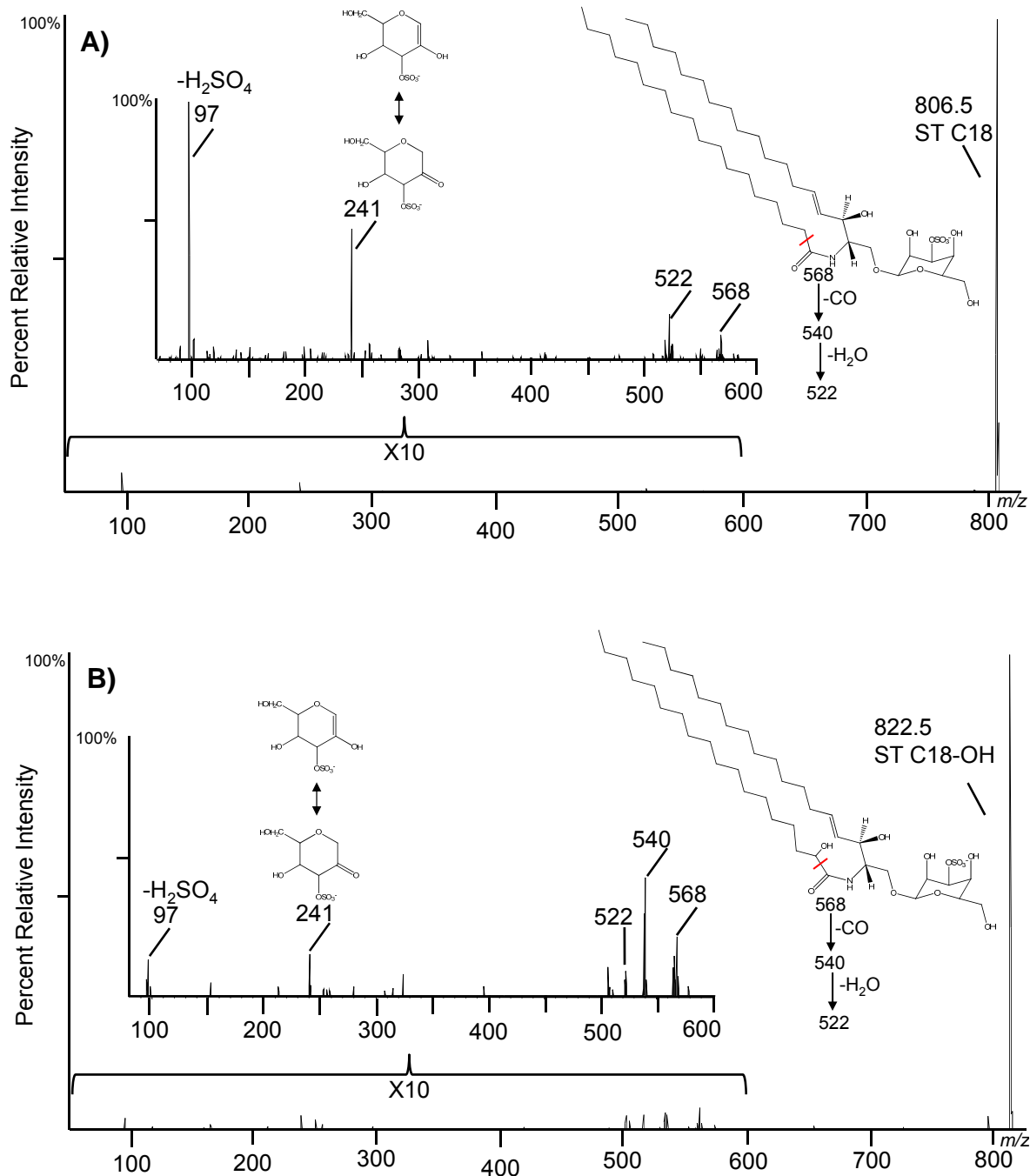
Supplemental Figure 7



Supplemental Figure 7. On-tissue fragmentation of ganglioside GM1a (1544.8) by MALDI linear ion trap (Thermo Scientific, Waltham, MA, USA). Neu5Aca2–3(Galb1–3GalNAcb1–4)Galb1–4Glc1–1Cer or as II3Neu5AcGg4Cer. A) Fragmentation of peak 1544.4, GM1a precursor; B) MS³ products from m/z 1253.4 and 888.5.

Abbreviations: GA1- Galβ1-3GalNAcb1-4Galβ1-4Glcβ1-1Ceramide ; CDH-Galβ1-4Glcβ1-1Ceramide; GM3-Gal3-(2aNeuAc)β1-4Glcβ1-1Ceramide; Glc- glucose.

Supplemental Figure 8



Supplemental Figure 8. Fragmentation of sulfatides using pulsed Q dissociation with a MALDI linear ion trap (Thermo Scientific, Waltham, MA, USA). A) Fragmentation of C18 sulfatide (3'-sulfo)Gal β -Cer(d18:1/18:0) at m/z 806.5; B) Fragmentation of C18-OH sulfatide ((3'-sulfo)Gal β -Cer(d18:0/2-OH-18:0) at m/z 822.5. Fragmentation patterns match those reported by Hsu et al in *Biochim Biophys Acta*, 1998, 1392 (2-3):202-216.